Seamless variation of isometric and anisometric dynamical integrity measures in basins's erosion

Seamless variation of isometric and anisometric dynamical integrity measures in basins's erosion

P. Belardinelli[a,b,*], S. Lenci[b], G. Rega[c]

[a] *Precision and Microsystems Engineering, TU Delft, Delft, The Netherlands*
[b] *DICEA, Polytechnic University of Marche, Ancona, Italy*
[c] *DISG, Sapienza University of Rome, Rome, Italy*

Abstract

Anisometric integrity measures defined as improvement and generalization of two existing measures (LIM, local integrity measure, and IF, integrity factor) of the extent and compactness of basins of attraction are introduced. Non-equidistant measures make it possible to account for inhomogeneous sensitivities of the state space variables to perturbations, thus permitting a more confident and targeted identification of the safe regions. All four measures are used for a global dynamics analysis of the twin-well Duffing oscillator, which is performed by considering a nearly continuous variation of a governing control parameter, thanks to the use of parallel computation allowing reasonable CPU time. This improves literature results based on finite (and commonly large) variations of the parameter, due to computational constraints. The seamless evolution of key integrity measures highlights the fine aspects of the erosion of the safe domain with respect to the increasing forcing amplitude.

Keywords: Basins of attraction, dynamical integrity, anisometric measures, basin erosion, system safety

1. Introduction

In nonlinear dynamics the possible coexistence of multiple attractors for a given system is well known and, indeed, it represents the common situation named multistability [1, 2, 3]. A generic attractor, be it a stationary (equilibrium) point, a limit-cycle, a quasi-periodic or a chaotic motion, can be detected by inspecting orbits of the system as the time goes to infinity. Its basin of attraction is the subset of the phase space, i.e. the set of initial conditions, that converges to it forward in time. Because of multistability, the phase space is the union of various basins of attraction, one per attractor, which do not intersect with each other, since the forward evolution in time is unique [4].

By modifying the system parameters the position of attractors change, and they can also bifurcate leading to different attractors. Related basins of attraction are altered as well: basins deform and reshape, new ones can appear or existing be destroyed. Even if system parameters slightly change, a rapid erosion or a stratification of the basin can occur [5, 6], often as a consequence of homoclinic intersection of stable and unstable manifolds [4].

A basin can be a substantially large region of the phase space but, if its structure is highly intertwined or characterized by fractal boundaries, with a "small" compact part around the attractor,

*Corresponding author: Pierpaolo Belardinelli, Department of Precision and Microsystems Engineering, Research group of Micro and Nano Engineering, 3ME, Mekelweg 2, (2628 CD) Delft, The Netherlands. Email: p.belardinelli@tudelft.nl

the long-term predictability depends on uncertainties in the initial conditions specification [7]. In this case, the stability of an attractor in classical Liapunov's sense, i.e. against infinitesimal disturbances, does not have a practical engineering validity as noisy environments and imperfections must be accounted for. The "practical stability" is needed instead of the "theoretical stability", and the safety of the system is related to the capability to accommodate "moderate" (small but not infinitesimal) perturbations without undesired consequences [8].

The loss of engineering robustness due to larger excitations has been analyzed in the fundamental work of Thompson [9]. The concept of dynamical integrity is therein introduced and applied to a mechanical oscillator where the escape from a cubic potential well beyond the hilltop saddle is presented. Several works have then examined the erosion of basins of attraction by focusing on the practical stability reduction and the consequent vulnerability to disturbances. The contact of a single-well attractor in the twin-well Duffing oscillator with the boundaries of its basin is examined in [10]. The control, shift and reduction of the erosion of the basins of attraction has been studied with the aim of the elimination of homoclinic tangencies and regularization of fractal basins both in macro [11] and micro systems [12].

The estimation of the safety of basins of attraction plays a key role in a system design. The issue has been addressed by Soliman and Thompson [13] and in the last years Rega and Lenci [14] investigated different measures able to quantify an admissible set of initial conditions of the phase space.

In dynamical integrity analyses it is crucial to study how the basins of attraction, and their integrity measures, evolve by varying a parameter of the system. This provides the so-called *integrity profiles* [15, 16], that are very helpful in understanding the degradation of robustness, and allow to fix some thresholds for safety.

Drawing integrity profiles requires building many basins of attractions, and thus it is very time consuming. It is for this reason that integrity profiles are usually built only for "discrete" values of the varying parameter. While being sufficient for an overall understanding of the system behaviour, this misses some important aspects of the dynamics like, for example, sudden jumps (due to the appearance of a new attractor inside the basin of a previous attractor) and locally strange behaviours (commonly related to minor or rare attractors [17, 18]). It is thus extremely useful to have seamless integrity profiles, which provide information otherwise lost.

This is the first goal of this paper, where "continuous" curves are obtained by building a huge number of basins of attraction. This has been possible, in reasonable time, by using high performance computation, and in particular parallel computing, adopting in the present analysis algorithms developed by the authors for elaborating basins of attractions of high dimensional systems [19, 20].

In previous works perturbations of initial conditions in displacement and velocity are assumed to be equally important, and are then considered of the same level. In fact, previously proposed (isometric) integrity measures do not distinguish between displacement and velocity, or more generally between different coordinates in phase space. However, it may happen that a system is more susceptible, say, to velocity rather than to displacement, e.g. under the presence of an impulsive excitation. It is thus useful to introduce measures that take into account this aspect. As a byproduct, this allows us to better deal with mechanical degrees of freedom (displacements vs velocities) that have different physical dimensions, being thus affected by the choice of the system of measurement. This is the second goal of this paper. Anisometric integrity measures weighting in a different way each coordinate of the phase space are introduced and deeply investigated.

Both seamless integrity profiles and the performance of different integrity measures are investigated with reference to the global dynamics of a two-well bistable Duffing oscillator. The paper is

organized as follows. Anisometric integrity measures are defined in Sect. 2 as generalization of the underlying isometric ones. The considered paradigmatic model is illustrated in Sect. 3. Seamless variation of all measures for competing resonant and non-resonant attractors of the two-well Duffing oscillator is comparatively addressed in Sect. 4, by dwelling on their features and capability to identify regions of the phase space with predictable outcomes. In particular, their evolution in a 3D phase-parameter space is addressed in Sect. 5. The last section draws some conclusions and hints for future developments.

2. Isometric and anisometric dynamical integrity measures

If not preliminarily defining/identifying an actual safe basin, as discussed in [8, 14], the most straightforward integrity measure of a basin of attractor is represented by the Global Integrity Measure (*GIM*), namely by its hyper-volume, that reduces to an area in 2D problems. The *GIM* cannot be deemed a prudent indicator because it accounts for both compact and fractal, i.e. dynamically non-integer, parts of the basin. A more refined measure able to get rid of the unsafe fractal tongues from the integrity evaluation is the Integrity Factor (*IF*) [14]. The IF considers only the compact part of the basin and calculates the largest hyper-sphere within (circle in 2D cases). A more conservative measure is represented by the Local Integrity Measure (*LIM*), whose definition retraces the IF, being again the radius of the largest hyper-sphere entirely contained in the basin but constrained to be centred at the attractor of reference. A less used measure, expression of the safe attractor stability, is the impulsive integrity measure (*IIM*). It is the distance between the attractor and the nearest boundary of the basin along the direction related to the generalized velocity. $IIM^{\pm}$ indicates the minimum of the distances along positive (IIM^{+}) and negative (IIM^{-}) directions.

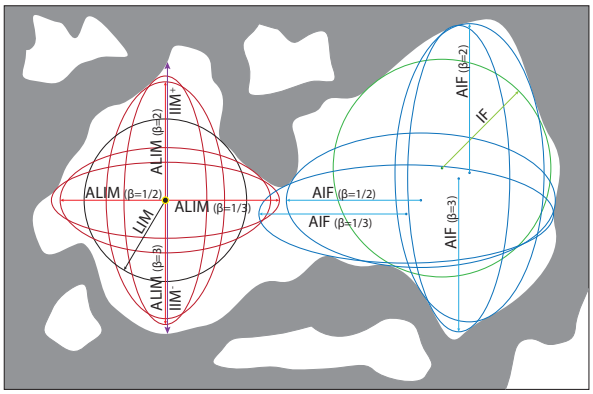

Figure 1: Example of an overall hypothetical attractor-basin phase portrait with the illustration of the integrity measures. The black spot on the left part of the figure represents the considered attractor.

As it can be perceived, all the aforementioned measures do not account for inhomogeneous sensitivities of the state space variables but, in practical applications, a system could be primarily affected by perturbations in one of its characteristic quantities (e.g. velocity, position, etc.). The local integrity measure is thus generalized with the introduction of the *Anisometric Local Integrity Measure* (*ALIM*) that is non-equidistant in the state-space coordinates. It is defined as the maximum of the two semi-axes of an ellipse centred in the safe attractor and totally contained in the largest compact (i.e. safe) portion of the basin. As a matter of fact, since integrity measures are commonly normalized to the same "initial" values, considering the length of the minor semi-axis or the area of the ellipse is equivalent to the assumed definition.

The *ALIM* requires to *a priori* fix the ratio between the axes of the ellipse along, e.g., the velocity and displacement directions, here denoted by β and called *anisometric parameter*; this reflects the different sensibility we have along the two directions. If $\beta = 1$ the *ALIM* reduces to the *LIM* while $\beta = 0, \infty$ describes a measure solely accounting for either one of the two generalized coordinates, e.g. *IIM* for $\beta = \infty$. We can alternatively use $\alpha = \arctan(\beta)$, which ranges in $[0, \pi/2]$ and does not assume infinite values.

Analogous definition can be formulated for the *Anisometric Integrity Factor* (*AIF*) with the due differences. The center of the *AIF*, as in the *IF*, is not constrained in the basin attractor and, thus, it is "free" to move within the basin accommodating jagged surfaces. Again, the measure corresponds to the maximum of the two semi-axes of the biggest ellipse totally contained in the safe basin. Finally, the *AIF* is the *IF* for $\beta = 1$. In Figure 1 a separate illustration of the described measures is reported over an overall hypothetical attractor-basin phase portrait. It is worth to note that the integrity measures are usually normalized with respect to a reference value. However, the measures reported in this work have not been rescaled in order to facilitate the comparison with respect to the phase-space dimensions, especially for the anisometric cases.

The previous definitions of *ALIM* and *AIF* are valid in the 2D case. Extension to higher dimensional systems is straightforward, and requires fixing the ratios between all the N-axes of the hyper-ellipsoid in the N-dimensional phase space, according to the sensibility we have on each coordinate. Details of this extension are left for future works.

3. Dynamic model

Based on the outlined framework, the global dynamics of the two-well/bistable Duffing oscillator is investigated. This archetypical system is able to describe many nonlinear systems and it is a powerful model to study qualitatively several nonlinear behaviours; the governing equation is (see eq. (7.1.2) of [21])

$$\ddot{y} + 2\zeta\dot{y} - y + \gamma y^3 = f\cos(\Omega t), \tag{1}$$

which in the state space formulation becomes

$$\begin{cases} \dot{q}_1 = q_2, \\ \dot{q}_2 = -2\zeta q_2 + q_1 - \gamma q_1^3 + f\cos(\Omega t). \end{cases} \tag{2}$$

For the present analysis a linear viscous damping $\zeta = 0.025$ is considered, whereas other constant parameters are $\gamma = 1$, $\Omega = 1.2$ (as in Fig. 7.12(b) of [21]). The state space $\{q_1, q_2\}$, describing all the possible pairs {position, velocity} for the oscillator, is here limited to $q_{1,2} \in [-2, 2]$ and a square grid composed of 500^2 cells is considered for its discretization. A parametric variation, with respect to the excitation amplitude ($f \in [0.02, 0.135]$), is performed with a small step $\Delta f = 0.000254154$; this step is so small that practically we are performing a "continuous" analysis of the system for varying f. However, being this methodology computationally expensive, it can be systematically applied only if implemented by means of efficient and targeted algorithms, e.g. parallel computing, able to exploit the best performances of recent computational architectures [19, 20].

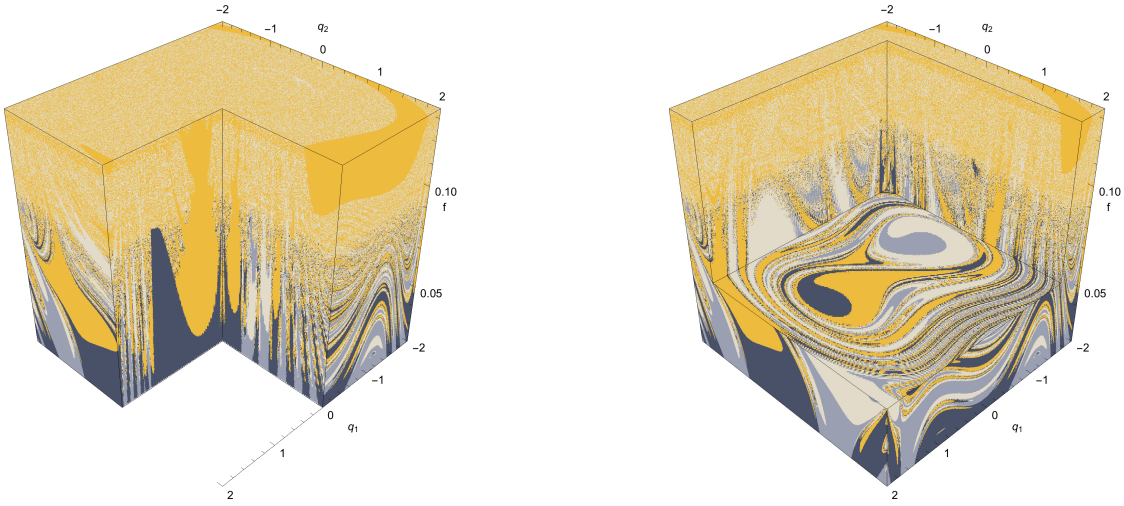

Figure 2: Sliced 3D views of the domain of parametric variation of basins of attraction.

Figure 2 shows stacks of basins of attraction in three-dimensional graphics. It is here underlined that only 2D sections with $f = const$ are proper basins of attraction. Both Figure $2(a)$ and Figure $2(b)$ are carved to illustrate basins's evolution as function of the excitation amplitude. The considered varying parameter f disrupts progressively the domains, bringing them to assume a fractal configuration. Furthermore, the continuous metamorphosis of basins shown in Figure 2 represents a new useful feature for the determination of safe working regions and critical thresholds towards dynamically non-integer domains.

4. Seamless variation of dynamical integrity measures

In this section we undertake an integrity analysis of the basins portraits by evaluating four different measures, namely the LIM, the $ALIM$, the IF and the AIF. Integrity profile curves for the left and right attractors of the considered system are reported in Figure $3(a)$ and Figure $3(b)$, respectively.

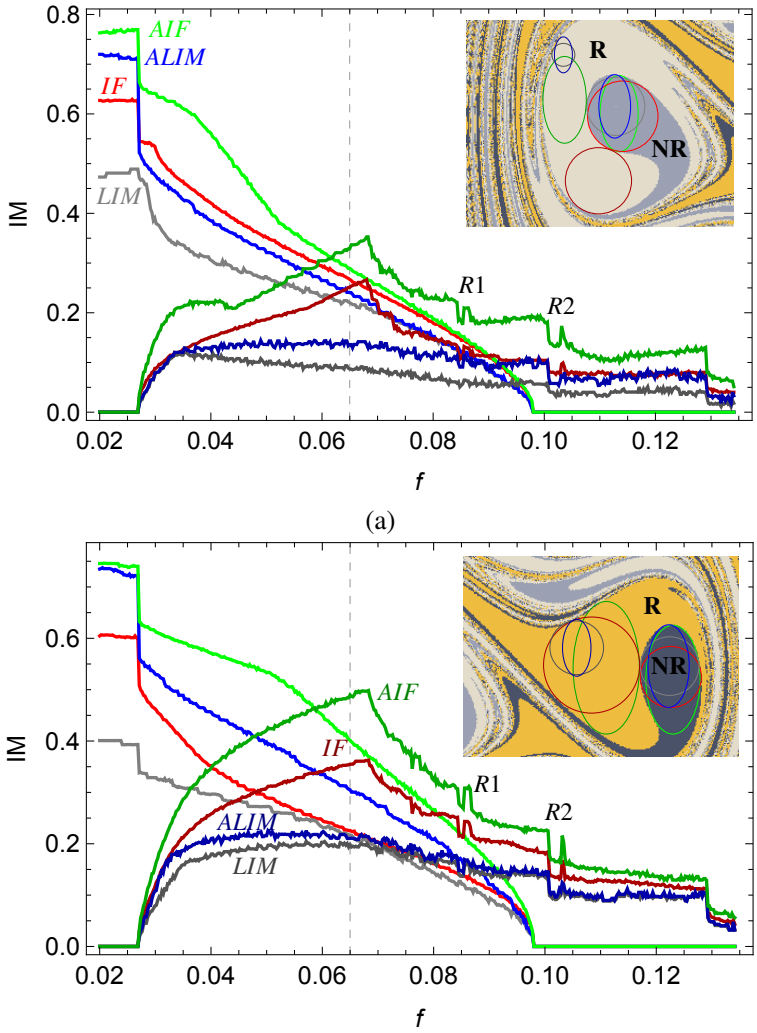

Figure 3: Integrity profile curves. The ratio for the anisometric measures is $\beta = 2$. The inset pictures show the shape of the integrity measures for $f = 0.0649853$. Darker colors of the curves refer to R-basins of large-amplitude (i.e. resonant) attractors. With the labels $R1$ and $R2$ are highlighted four drops in the measures due to rare attractors [17, 18]. a) Basin and measures for "left side" attractors. b) Basin and measures for "right side" attractors.

In each figure two sets of four curves depict integrity measures for the non-resonant (NR, small amplitude) and resonant (R, large amplitude) attractors, whose basins (with increasing excitation amplitude) in the two wells are decreasing and increasing, respectively. The lines referred to the small/large amplitude attractor end/start with null values. Four measures are reported: IF (red/dark red), $ALIM$ (blu/dark blu), LIM (gray/dark gray), AIF (green/dark green). A decreasing/increasing trend is reflected in a reduction/increment of dynamical integrity of the system. The curves reported in Figure $3(a)$ and Figure $3(b)$ show similarity in their behaviour. Measures connected with the small amplitude attractors present a first region where they are generally insensitive to the variation of the driving parameter f. Then, sudden drops of the integrity measure directly connected with the appearance of resonant attractors occur. Finally, an ever-decreasing trend corresponds to the non-resonant basins shrinking towards zero. Regards the basins of the resonant attractors, after their appearance, an alike behaviours can be recognized for the couples AIF/IF

and $ALIM/LIM$. Local integrity measures present an increasing trend only for a small portion in the variation range of the excitation amplitude, contrary to AIF/IF that have a more extended growing region. Moreover, it can be observed that the distance between anisometric ($ALIM$ or AIF) and corresponding isometric (LIM or IF) measures, for a fixed value of the parameter f, demonstrates how the different sensitivity on the generalized coordinates affects the evaluation of the integrity measure.

As a consequence of their definitions, for the anisometric measures the sorting $AIF \geq ALIM$ is always preserved, but we cannot draw conclusions about the sorting between $ALIM$ and IF, even if for their isometric subfamilies is $IF \geq LIM$. The inset plot in both subfigures of Figure 3 illustrates that the $ALIM$ can be greater, equal or less than IF. Indeed the reported basins for $f = 0.0649853$ present a value for the small amplitude attractors in the two wells with $ALIM$ less or greater than the IF, whereas for the large amplitude attractors it is always $IF > ALIM$. Thus in the presented configuration with $\beta = 2$, for the large amplitude attractor the non-equidistant measure results more conservative. Furthermore, it can be noted that AIFs present the largest values for all the considered attractors. This is a consequence of the fact that the basins of attraction are somehow stretched in the vertical direction, as can be seen from the insets in Figure 3; thus, this property is no longer true if we assume $\beta < 1$.

To practically compute the anisometric (isometric) integrity factor AIF (IF), we considered all points of a given basin of attraction B. For each point P we determined the largest $\beta = 2$ ellipse (circle) *centered in P* and tangent to the basin boundary ∂B, and measured its maximum semi-axis (radius) $R = R(P)$. The AIF (IF) is just, by definition, the largest value of R for varying point P within the basin, $AIF/IF = max_{P \in B}\{R(P)\}$. This algorithm stresses the fact that AIF (IF) is a property of the whole basins of attraction. It is worth to remark that this algorithm is not needed in the computation of $ALIM$ (LIM), since in this case the center of the ellipse (circle) is fixed - it is the attractor.

While not being the integrity factor, it can be useful to draw the function $R(P)$ in order to have a measure of the sensitivity to imperfections of the various parts of the given basin of attraction. This permits to evaluated the safety of the subsets of B.

Drawing all together the functions $R(P)$ of each basin of attraction can help to identify safe and, mostly, reliable, regions in the phase space where the system outcome is totally predicted. For $f = 0.0581232$ this has been done in Figure 4(a) for the AIF and in Figure 4(b) for the IF.

The ellipses (circle) corresponding to the AIF (IF) of the 4 basins of attraction are also reported in Figure 4(a) (Figure 4(b)): it is immediate to check that they are centered in the points with the highest $R(P)$, according to the definitions of the integrity factors.

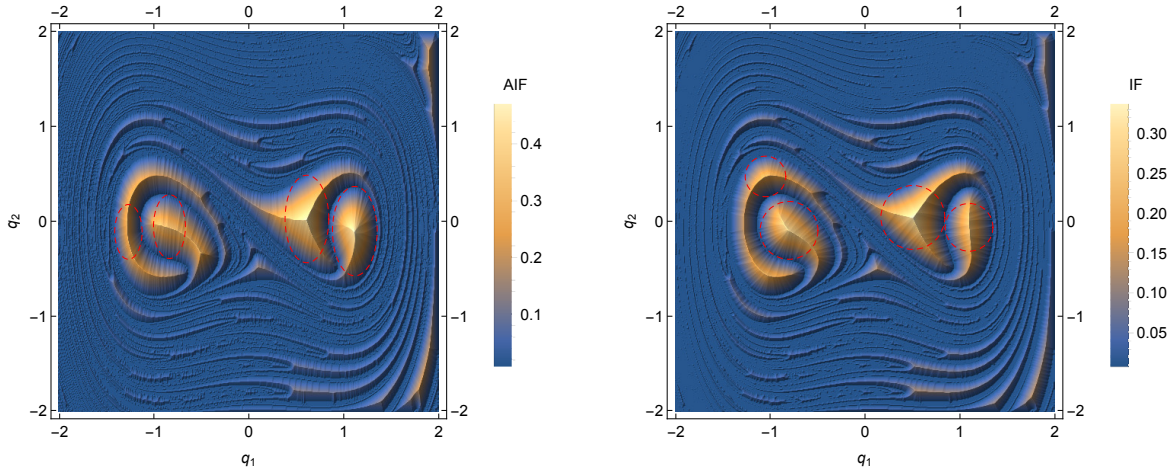

(a) (b)

Figure 4: Density plots illustrating the distribution of the $R(P)$ function over the entire domain for $f = 0.0581232$. Red dashed ellipses/circles indicate the maximum values of the measures, corresponding to a) AIF ($\beta = 2$) and b) IF.

The use of algorithms to determine simultaneously the evolution of the basins is an appealing feature, which overcomes the usual analyses based on discrete (and commonly spread) values of the parameter or focused only on the variation of the basin boundaries with respect to a starting basin. A nearly continuous approach also permits to catch quite easily the presence of rare attractors [17, 18]. Two rare attractors, designated as $R1$ and $R2$ within the Figure 3, responsible for a local reduction of the system integrity, are reported in Figures 5 and 6 (the evolving green tongues with red attractors). Commonly rare attractors, while being interesting from theoretical point of view, are not *directly* important from a practical point of view, as they exist in very narrow ranges of the parameter space. However, their *indirect* effects could be very important; for example, as a consequence of various heteroclinic intersections, they may be responsible for the fractalization - and thus reduction of the dynamical integrity - of basins of major attractors. For this reason they must be carefully investigated in any case [22]. In particular, the computation of dynamical integrity measures in presence of rare attractors highlights sudden, yet localized, variations in the measures and a consequent reduction of the inner safety of the system. For all this, an adequate resolution in the parametric study is required in order to avoid an overlook of cells belonging to unsafe basins.

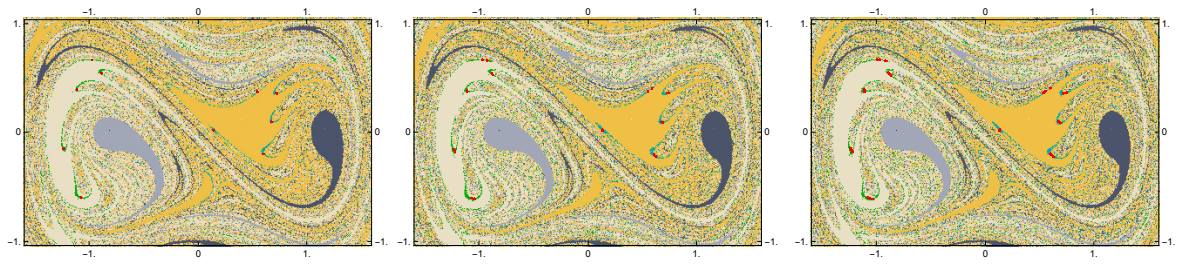

(a) (b) (c)

Figure 5: Basins of attraction with the appearance, evolution and disappearance of left and right rare attractors ($R1$). a) Period-5 $R1$ attractors ($f = 0.084809$). b) Period-10 $R1$ attractors ($f = 0.085318$) . c) Period-20 $R1$ attractors just before their disappearance ($f = 0.085445$).

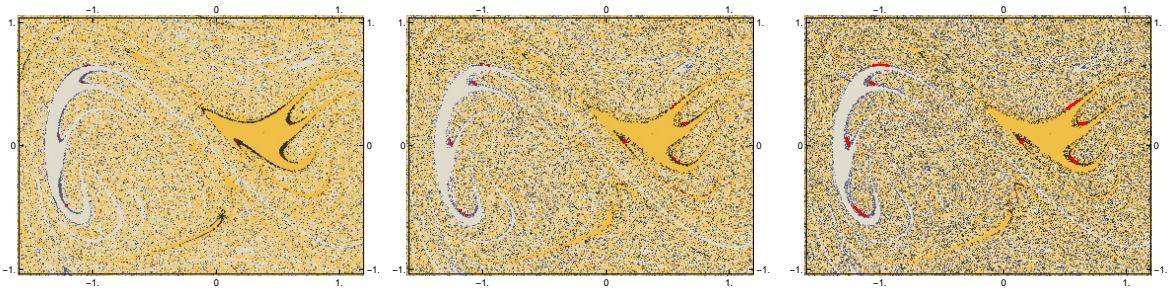

(a) (b) (c)

Figure 6: Basins of attraction with the appearance, evolution and disappearance of left and right rare attractors ($R2$). a) Period-4 $R2$ attractors ($f = 0.0100821$). b) Period-8 $R2$ attractors ($f = 0.01026$). c) $R2$ attractors just before their disappearance ($f = 0.0102854$).

In Figure 7 is reported the variation of the *ALIM* with respect to the β ratio. The curves below the *LIM* (red curve with $\beta = 1$) are obtained with a ratio less than the unit ($\beta = 1/2, 1/3$). Since the shape of the basins is stretched along the q_2 coordinate, this results in small measures limited by the contact with other basins along q_1. The integrity measure shows a convergence, by increasing the β ratio ($\beta = 1.2, 1.5, 2, 3$), indeed only a shallow discrepancy can be detected in between $ALIM_{\beta=2}$ and $ALIM_{\beta=3}$, although more remarkable in the resonant attractors.

In the present approach the anisometric parameter β is fixed a priori, thus reflecting our perception on the different sensitivity to variations of different state space variables. The fact that in the present case *ALIM* is practically an increasing function of β means that the system is more sensitive to the q_1 variable, as confirmed by the fact that, in general, the basins are stretched along the q_2 (velocity) direction. This implies that for an actually safe system design it would be necessary to refer to the integrity profiles obtained with β less than unity.

A more comprehensive approach could be pursued, in which β is not fixed a priori, but left free during the integrity analysis. It can be, for example, the one providing the largest area of the involved ellipses. In this case, β would be a result of the analysis, so that the integrity evaluation would directly shed light on the different sensitivity of the considered system along different directions. The development of this idea is left for future work.

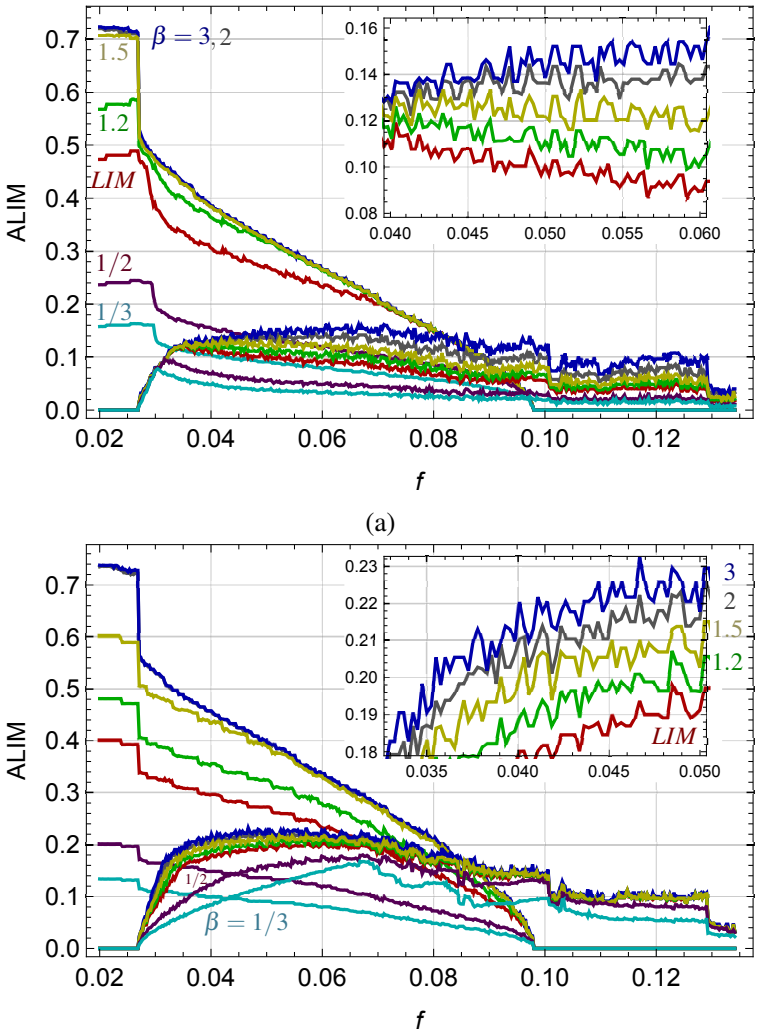

Figure 7: Variation of the *ALIM* with respect to the ratio β. In each subfigure 7 curves are reported with $\beta = 1/3, 1/2, 1, 1.2, 1.5, 2, 3$. a) *ALIM* for "left side" attractors. a) *ALIM* for "right side" attractors.

5. Evolution of integrity measures in a 3D phase-parameter space

Along with the integrity profiles, the full control of safe regions, in order to avoid overestimations, relies on the systematic metamorphoses evaluation of the measure in the phase/parameter-space. Three-dimensional sweeps for the considered integrity measures are shown in Figures 8 and 9. In each subplot an inset above-orthographic view visualizes the evolution of the attractors position in the phase plane up to their disappearance.

Figure $8(a)$ and Figure $8(b)$ compare the local integrity measure in the isometric and anisometric version, respectively. It can be observed the sudden reduction of the values for the non-resonant attractors, reported in red and blue blended colors, in connection with the appearance and growth of the resonant attractors (green and purple colors), which then also disappear over a longer parameter interval. Obviously the positions of the centres on both the cases are identical since they are bound to the attractor. On the contrary, the location of the centres for IFs and AIFs can differ sensibly as reported in Figure 9. Moreover, the evolution is only piecewise connected, thus, to an

optimal integrity profile curve can be associated to a spread dislocation of the measure within the compact part of the basin, as it can be noticed mostly for the green and purple resonant basins. The characterization of safe working regions based on three-dimensional integrity manifolds, as illustrated in Figures 8 and Figures 9 is an added-value to the mere integrity profiles. Indeed, it evaluates the magnitude of the integrity measure, combined with its actual space localization, as function of a design parameter.

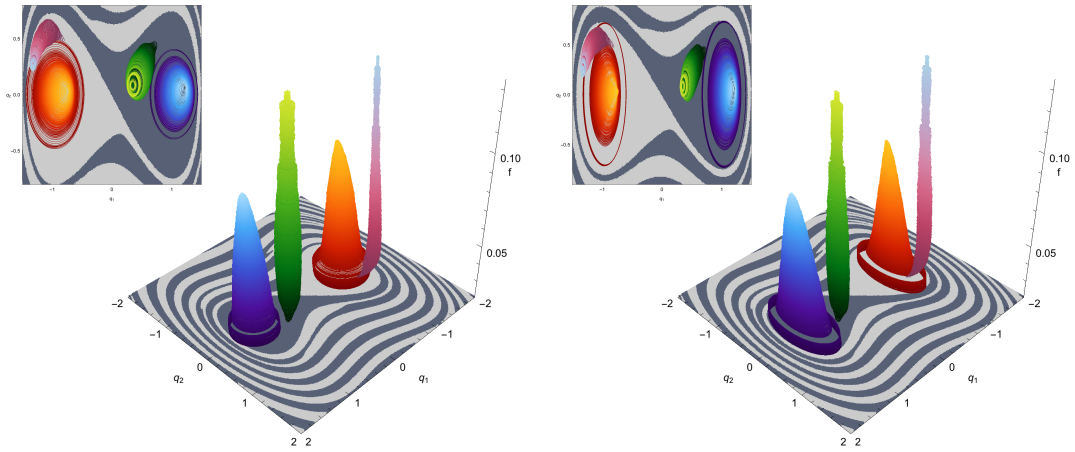

(a) (b)

Figure 8: 3D variation of the local integrity measures for both left and right attractors. The above-orthographic view is shown in the upper side inserted pictures. a) LIM. b) $ALIM$ ($\beta = 2$).

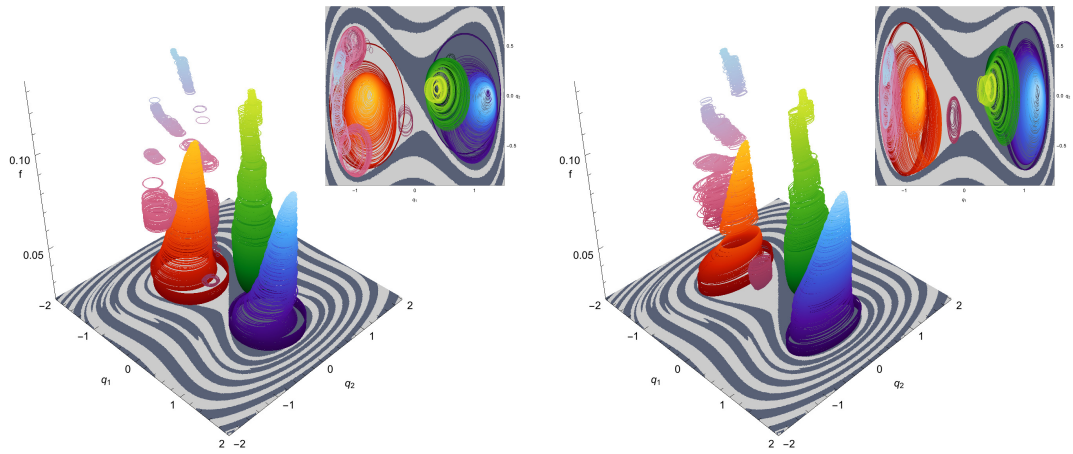

(a) (b)

Figure 9: 3D variation of the integrity factors for both left and right attractors. The above-orthographic view is shown in the upper side inserted picture. a) IF. b) AIF ($\beta = 2$).

6. Conclusions

The generalization of two existing dynamical measures, namely the local integrity measure and the integrity factor, has been proposed with their anisometric extensions. The introduced measures are able to identify properly a different sensitivity of the generalized coordinates to a parameter variation. To illustrate the new concepts, a study of the global dynamics of the two-well/bistable

Duffing oscillator has been presented. A parametric investigation with respect to the external excitation amplitude has been performed with a reduced step size, getting a nearly seamless evolution of integrity measures. By means of three dimensional plots, illustrating the basins erosion through the distribution of the integrity measures in phase-space with respect to the driving parameter, a better visualization and identification of safe regions has been achieved.

The presented idea of anisometric dynamical integrity measures will be extended to higher dimensional systems in future developments. Furthermore, new insights can be deduced from the analysis of basins by using unfixed anisometric grades. Thus, the different sensitivity of the system to specific perturbations can come up as result of the evolution of anisometric parameters.

Acknowledgement

The authors wish to thank Prof. Marian Wiercigroch for discussions on anisometric integrity measures.

References

[1] U. Feudel. Complex dynamics in multistable systems. *International Journal of Bifurcation and Chaos*, 18(06):1607–1626, 2008.

[2] U. Feudel, C. Grebogi, L. Poon and J.A. Yorke. Dynamical properties of a simple mechanical system with a large number of coexisting periodic attractors. *Chaos, Solitons & Fractals*, 9(1):171 – 180, 1998.

[3] R. Dieci, G.I. Bischi and L. Gardini. Multistability and role of noninvertibility in a discrete-time business cycle model. *Central European Journal of Operation Research*, 9:71–96, 2001.

[4] S. Wiggins. *Introduction to Applied Nonlinear Dynamical Systems and Chaos*. Texts in Applied Mathematics. Springer, 2003.

[5] M.S. Soliman and J.M.T. Thompson. Global dynamics underlying sharp basin erosion in nonlinear driven oscillators. *Phys. Rev. A*, 45:3425–3431, Mar 1992.

[6] J.M.T. Thompson and M. S. Soliman. Fractal control boundaries of driven oscillators and their relevance to safe engineering design. *Proceedings of the Royal Society of London A: Mathematical, Physical and Engineering Sciences*, 428(1874):1–13, 1990.

[7] C. Grebogi, S.W. McDonald, E. Ott and J.A. Yorke. Final state sensitivity: An obstruction to predictability. *Physics Letters A*, 99(9):415 – 418, 1983.

[8] G. Rega and S. Lenci. A global dynamics perspective for system safety from macro- to nanomechanics: Analysis, control, and design engineering. *Applied Mechanics Reviews*, 67(5):050802–050802, 10 2015.

[9] J.M.T. Thompson. Chaotic phenomena triggering the escape from a potential well. *Proceedings of the Royal Society of London A: Mathematical, Physical and Engineering Sciences*, 421(1861):195–225, 1989.

[10] A.N. Lansbury, J.M.T. Thompson and H.B. Stewart. Basin erosion in the twin-well Duffing oscillator: Two distinct bifurcation scenarios. *International Journal of Bifurcation and Chaos*, 02(03):505–532, 1992.

[11] S. Lenci and G. Rega. Optimal control of nonregular dynamics in a Duffing oscillator. *Nonlinear Dynamics*, 33(1):71–86, 2003.

[12] S. Lenci and G. Rega. Control of pull-in dynamics in a nonlinear thermoelastic electrically actuated microbeam *Journal of Micromechanics and Microengineering*, 16(2): 390 – 401, 2006.

[13] M.S. Soliman and J.M.T. Thompson. Integrity measures quantifying the erosion of smooth and fractal basins of attraction. *Journal of Sound and Vibration*, 135(3):453 – 475, 1989.

[14] G. Rega and S. Lenci. Identifying, evaluating, and controlling dynamical integrity measures in non-linear mechanical oscillators. *Nonlinear Analysis: Theory, Methods & Applications*, 63(5-7):902 – 914, 2005.

[15] S. Lenci and G. Rega. Competing dynamic solutions in a parametrically excited pendulum: Attractor robustness and basin integrity. *Journal of Computational and Nonlinear Dynamics*, 3(4):041010–041010–9, 09 2008.

[16] S. Lenci and G. Rega. Load carrying capacity of systems within a global safety perspective. Part II. attractor/basin integrity under dynamic excitations. *International Journal of Non-Linear Mechanics*, 46(9):1240 – 1251, 2011.

[17] A. Chudzik, P. Perlikowski, A. Stefanski and T. Kapitaniak. Multistability and rare attractors in van der pol- duffing oscillator. *International Journal of Bifurcation and Chaos*, 21(07):1907–1912, 2011.

[18] A. Klokovs and M. Zakrževskis. Bifurcation analysis and rare attractors in driven damped pendulum systems. *Journal of Vibroengineering*, 12:369–374, 2010.

[19] P. Belardinelli and S. Lenci. An efficient parallel implementation of cell mapping methods for mdof systems. *Nonlinear Dynamics*, 86(4):1–12, 2016.

[20] P. Belardinelli and S. Lenci. A first parallel programming approach in basins of attraction computation. *International Journal of Non-Linear Mechanics*, 80:76–81, 2016.

[21] S. Lenci and G. Rega. Forced harmonic vibration in a Duffing oscillator with negative linear stiffness and linear viscous damping. In I. Kovacic and M.J. Brennan, editors, *The Duffing Equation*, Chapter 7, pages 219–276. John Wiley & Sons, Ltd, 2011.

[22] M. Zakrževskis. New concepts of nonlinear dynamics: Complete bifurcation groups, protuberances, unstable periodic infinitiums and rare attractors. *Journal of Vibroengineering*, 10:421–441, 2008.